Journal of Sound and Vibration 434 (2018) 28–43

Contents lists available at ScienceDirect

Journal of Sound and Vibration

journal homepage: www.elsevier.com/locate/jsvi

Experimental and analytical investigation on sound transmission loss of cylindrical shells with absorbing material

Pouria Oliazadeh [a], Anooshiravan Farshidianfar [a,*], Malcolm J. Crocker [b]

[a] Department of Mechanical Engineering, Ferdowsi University of Mashhad, Mashhad, Iran
[b] Department of Mechanical Engineering, Auburn University, Auburn, AL 36849, USA

ARTICLE INFO

Article history:
Received 10 December 2017
Revised 6 July 2018
Accepted 8 July 2018
Available online XXX
Handling Editor: R.E. Musafir

Keywords:
SEA theory
Sound intensity method
Sound transmission loss
Transmission suite method

ABSTRACT

In this study, sound transmission through a thin-walled cylindrical shell is investigated both analytically and experimentally. A theoretical model based on statistical energy analysis (SEA) is developed in order to calculate the noise reduction and sound transmission loss of the cylindrical shell. The procedure to obtain the parameters involved in the SEA model, such as radiation efficiency and loss factors, is explained in detail. An experimental setup was constructed in a reverberation chamber to evaluate the transmission loss of the cylinder using two experimental methods. First the transmission suite method which includes measurements of the sound pressure levels inside and outside of the cylinder using microphones was used. Then the sound intensity method was used in which the transmitted sound intensity is measured with a sound intensity probe. The experimental results are compared with the analytical results obtained from the SEA theory, which shows good agreement. By comparing both experimental techniques, the transmission suite method is found to have advantages over the other method at low frequencies. However, the sound intensity method is more applicable in the medium and high frequency regions between the ring and critical frequencies in order to predict the noise transmission characteristics of the cylindrical shell. Another experiment was conducted with absorbing materials placed inside the cylinder. The use of sound absorbing material produced a significant reduction in the noise level in the cylinder specifically in the high frequency range. The effects of the absorption coefficient on the acoustical behavior of the cylindrical shell were also investigated theoretically.

1. Introduction

Thin cylindrical shells have a wide variety of applications in many engineering structures such as car bodies, buildings, ship hulls and aircraft fuselages. Therefore, abating interior noise levels has a high priority in the design of engineering structures. Since increasing the mass of a structure for sound insulation is not easily applicable and has a direct effect on the final cost and in some cases on fuel consumption, using light-weight sound absorbing materials such as fiberglass is helpful and effective.

The sound insulation performance of a cylinder may be evaluated from a knowledge of its sound transmission loss, which is the ratio of the incident sound energy to the transmitted sound energy expressed in decibels [1]. Thus, a better understanding of the acoustical properties of cylinders is essential in order to achieve good noise attenuation. Reducing the vibration of thin cylindrical shells and interior noise levels produced is an important research topic. Analytical methods can be categorized into methods based on infinite cylinder models and methods based on finite models.

* Corresponding author.
E-mail address: farshid@um.ac.ir (A. Farshidianfar).

https://doi.org/10.1016/j.jsv.2018.07.017
0022-460X/

Koval [2–4] has presented a mathematical model for an infinitely long cylindrical shell in order to study the transmission of airborne noise into an aircraft fuselage. Blaise et al. [5] developed Koval's expression for an orthotropic infinite shell. Blaise and Lesueur [6] investigated the transmission loss of two-dimensional multi-layered infinite cylindrical shells. Lee and Kim [7–9] studied the sound transmission characteristic of single- and double-walled thin shells and stiffened structures. They used an infinitely long circular cylindrical shell model which was subjected to an acoustic wave and analyzed the effect of different design parameters on the sound transmission loss of the shell. Zhou et al. [10,11] modeled porous material in infinite double-walled panels and shells and obtained the transmission loss by considering the effect of external mean flow. Their results were then discussed by Liu and He [12]. Liu and He [13] studied sound transmission through double-walled sandwich shells with poroelastic cores. They showed that poroelastic core can improve the sound insulation performance in the mass law region. Liu and He [14] also showed that the air flow affects acoustic transmission across double-walled sandwich shells. The triple-walled structures with poroelastic linings have better acoustic performance than the double-waled ones and the internal and external gap flows can be considered as design tools to control the noise level [15,16]. Oliazadeh and Farshidianfar [17] calculated the sound transmission loss for a triple-walled shell and compared the results obtained with a double-walled shell. The research works presented so far have considered an infinite model for the cylindrical shell and used the wave propagation approach for the analysis of sound transmission.

While the wave propagation approach is capable of predicting sound transmission through an infinite cylindrical shell, it does not take into account the effects of boundary conditions and damping of the structure. The statistical energy analysis (SEA) approach includes the effect of finite cylinder dimensions. Damping can be considered in the SEA method by modeling the coupling between cylinder and acoustic media inside and outside. The SEA method was developed by Maidanik [18], Lyon [19] and by Crocker and Price [20] for analyzing sound transmission through panels and partitions. They showed how a system that consists of several subsystems can be modeled using SEA. Each subsystem may receive an input power from an external source such as a shaker or a loudspeaker. The power flows from one subsystem to another and can also be dissipated because of damping in each subsystem. Wang et al. [21] used the SEA method to evaluate the sound transmission loss of a light aircraft fuselage modeled by an aluminum cylinder.

The internal loss factor, coupling loss factor and modal density are three SEA parameters required to predict the energy in each subsystem. Internal and coupling loss factors have been investigated by researchers for the sound transmission through a wall in between two rooms [22], across a floor [23] and through a thin cylindrical shell coupled to an end plate [24]. The modal density has also been evaluated for unstiffened [25,26], stiffened [27,28] and composite [29] cylindrical shells.

Hynna et al. [30] developed the SEA method by using the finite element method in order to predict the structure-borne sound transmission in large welded ship structures. Craik and Wilson [31] studied airborne transmission through a wall using the SEA method. Chronopoulos et al. [32] presented a model for the prediction of the vibroacoustic performance of composite shells using the SEA approach.

Besides analytical methods, experimental techniques have also been developed to measure the sound transmission loss of structures. Wang et al. [21] previously evaluated the transmission loss of an aluminum cylinder using two experimental methods, (1) the sound intensity technique and (2) the transmission suite method and compared them with the SEA result. The sound intensity technique has some advantages [33]. The essential parameters and conditions for the measurement of the transmission loss have been studied by several researchers [34–36]. Chen et al. [37] presented a technique to measure damping components of plate by the sound intensity method. Watts [38] developed an *in situ* method in order to determine the transmission loss of noise barriers. He considered the traffic as the source of noise and measured the incident and transmitted sound intensity. Praščević et al. [39] used the sound intensity method for measuring the transmission loss of lightweight partitions and compared the results with those obtained using different theoretical models. Connelly and Hodgson [40] investigated the sound transmission of vegetated roofs experimentally using the sound intensity method. They performed a series of field tests and measured the transmitted acoustic intensity in order to design the experimental setup. Koukounian and Mechefske [41] predicted the vibro-acoustic response of an aircraft fuselage which is excited by a turbulent boundary layer. They verified the results using the experimental transmission suite method following the ASTM and ANSI standards. The purpose of the current paper is to study the sound transmission in air conditioning ducts which are modeled as cylindrical shells, experimentally and analytically.

In the present work, a theoretical model is presented based on the SEA theory that includes the effects of internal losses in the cylindrical shell and sound absorption inside the cylinder. The sound transmission loss of the cylindrical shell is obtained analytically using SEA and experimentally by installing the cylinder in a reverberation room. The transmission loss of the cylinder was measured using two experimental methods, the transmission suite method and the sound intensity method. The experimental approach is similar to that of Wang et al. [21]. However, they used an aluminum cylinder as a model of small and light aircraft cabins. With aircraft fuselages and cabins, the main object is to protect the passengers from the external powerplant noise. In this paper, the experimental setup is conducted with a thin steel cylinder such as those used in air conditioning systems in buildings. Steel ducts are cheaper than aluminum and in buildings the weight of the duct is not a problem. In this case, the noise transmission from inside to outside is important since an important purpose is to prevent occupants of buildings near the ducts from being disturbed. Since the transmission loss can be measured from inside to outside the cylinder, the interior noise level is made very high and the sound field is almost reverberant at high frequencies. Steel cylinders are normally thinner than aluminum ones and present much greater experimental difficulties. This is because the critical frequency is driven in higher frequencies making the measurements much harder because at high frequency the transmission loss is increased as a result of mass law. Although, significant difficulties occurred during the experiment because of the need for very powerful loudspeakers to be able to produce enough sound and overcome the background noise at high frequencies, the results showed reasonable

agreement when compared to the analytical results. A comparison is also made between the experimental techniques and the advantages and disadvantages of each method are discussed. Another experiment was conducted in which the interior space of the cylinder was filled with absorbing material and its effect on the interior noise level was investigated analytically and experimentally.

2. Theoretical model

A thin circular cylindrical shell with radius R, constant wall thickness h and length L is considered for the analysis in this paper. The material properties of the shell are defined in terms of Poisson ratio ν, *invacuo* bulk mass density ρ and *invacuo* Young's modulus of elasticity E. Simply supported boundary conditions are assumed for both ends of the cylindrical shell. The cylindrical coordinate system (x, θ, z) is used in the analytical study. The x coordinate is in the axial direction of the shell and θ and z coordinates denote circumferential and radial directions, respectively. The dimensions and coordinate system are shown in Fig. 1.

2.1. Natural frequency of a cylindrical shell

The displacements in the longitudinal, circumferential and radial directions for a cylindrical shell, which is simply-supported at both ends, are denoted by $u(x, \theta, t)$, $v(x, \theta, t)$ and $w(x, \theta, t)$, respectively. They are given by Eq. (1) as follows:

$$u(x,\theta,t) = U\cos(\frac{m\pi x}{L})\cos(n\theta)\cos(\omega_{mn}t), \tag{1a}$$

$$v(x,\theta,t) = V\sin(\frac{m\pi x}{L})\sin(n\theta)\cos(\omega_{mn}t), \tag{1b}$$

$$w(x,\theta,t) = W\sin(\frac{m\pi x}{L})\cos(n\theta)\cos(\omega_{mn}t), \tag{1c}$$

where U, V and W are the amplitudes of displacements in longitudinal, circumferential and radial directions, respectively, m and n are integers and called longitudinal and circumferential mode numbers, respectively and ω_{mn} is the angular frequency of the (m, n) mode. Substituting the above displacement fields into the equations of motion of a cylindrical shell under a free vibration, leads to a set of homogeneous equations having the following matrix form:

$$\begin{bmatrix} C_{11} & C_{12} & C_{13} \\ C_{12} & C_{22} & C_{23} \\ -C_{13} & -C_{23} & C_{33} \end{bmatrix} \begin{Bmatrix} U \\ V \\ W \end{Bmatrix} = \begin{Bmatrix} 0 \\ 0 \\ 0 \end{Bmatrix}. \tag{2}$$

The equation of motion and the coefficient matrix $[C_{ij}](i, j = 1, 2, 3)$ for some common cylindrical shell theories can be found in Refs. [42] and [17]. The coefficient matrix for the Soedel theory is presented in the Appendix. For a nontrivial solution, the determinant of the coefficient matrix in Eq. (2) must be zero.

$$\det[Cij] = 0\ ; \quad i, j = 1, 2, 3. \tag{3}$$

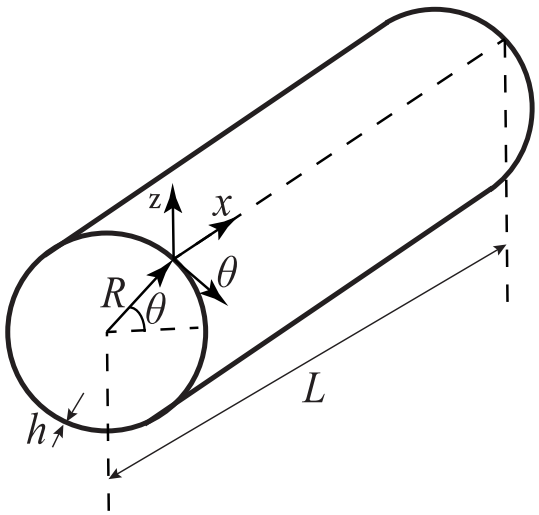

Fig. 1. Thin circular cylindrical shell: coordinate system and dimensions.

The expansion of Eq. (3) yields the frequency equation for the Soedel theory, having the following form:

$$\Omega^3 - C_2\Omega^2 + C_1\Omega - C_0 = 0, \tag{4}$$

where Ω represents the non-dimensional frequency parameter and is given by

$$\Omega = \frac{\rho(1-\nu^2)R^2}{E}\omega_{mn}^2. \tag{5}$$

and $C_i (i = 0, 1, 2)$ are the characteristic coefficients. In order to obtain a closed form solution for the natural frequencies, different assumptions can be made. Neglect of tangential inertia terms in the equations of motion reduces the frequency equation from a cubic form to a first order expression. By applying this procedure to the Soedel equations of motion, the following closed form solution for the non-dimensional frequency of a cylindrical shell, which is associated with a primarily radial motion, is obtained:

$$\Omega = \frac{A_1\lambda^2R^2 + A_2\lambda^4R^4 + A_3\lambda^6R^6 + A_4\lambda^8R^8 + A_5}{A_6\lambda^2R^2 + A_7\lambda^4R^4 + A_8}, \tag{6}$$

where $\lambda = m\pi/L$ and $A_i (i = 1, \ldots, 8)$ are functions of ν, n and $\beta = h^2/12R^2$ which are expressed as follows:

$$\begin{aligned}
A_1 &= \beta n^2(\frac{3}{4}\nu^2 - \frac{1}{2}\nu + \frac{5}{4}) + \beta n^3(n+1)(\nu-1) - 2\beta n^6(\nu-1) - \beta^2 n^4 - \beta^2 n^5(\nu+1) + \beta^2 n^6(\frac{1}{4}\nu^2 - \frac{3}{2}\nu + \frac{9}{4})\\
A_2 &= \beta n^2(\nu-1) - 3\beta n^4(\nu-1) + \beta^2 n^4(\frac{1}{2}\nu^2 - \frac{3}{2}\nu + 3) + \frac{1}{2}(1+\beta)(\nu-1)\nu^2 - 2\beta^2 n^3\\
A_3 &= -2\beta n^2(\nu-1) + \beta^2 n^2(\frac{1}{4}\nu^2 - \frac{3}{2}\nu + \frac{5}{4})\\
A_4 &= -\frac{1}{2}\beta(1+\beta)(\nu-1)\\
A_5 &= \frac{1}{2}\beta n^4(\nu-1) + \frac{1}{2}\beta^2 n^6(\nu-1) - \frac{1}{2}\beta(1+\beta)n^8(\nu-1)\\
A_6 &= n^2(\nu-1) - n^2\beta(\frac{1}{4}\nu^2 - \frac{1}{2}\nu + \frac{5}{4})\\
A_7 &= \frac{1}{2}(1+\beta)(\nu-1)\\
A_8 &= \frac{1}{2}(1+\beta)n^4(\nu-1).
\end{aligned} \tag{7}$$

Besides the natural frequencies of a cylindrical shell, there are two important frequencies that play a significant role in the acoustical behavior of a cylinder. These frequencies are called the ring and critical frequencies. The ring frequency, f_r is the lowest frequency at which a structural breathing mode resonance can occur. The second important frequency of a cylindrical shell, the critical frequency, f_c, occurs when the trace wavenumber in the radial direction matches the circumferential wavenumber of the shell. The ring and critical frequencies are given by Refs. [11,43]

$$f_r = (\frac{1}{2\pi R})\sqrt{\frac{E}{\rho}}, \tag{8a}$$

$$f_c = \frac{\sqrt{12}c_a^2}{4\pi^2 hRf_r}, \tag{8b}$$

where c_a is the speed of sound in air.

2.2. SEA model

In the SEA method, complex structures are divided into a number of subsystems which are linearly coupled together [19]. The behavior of the entire system can be predicted by modeling the coupling between subsystems. The total amount of energy input to each of the subsystems comes from external sources, which are usually random, is equal to the energy dissipated by mechanical damping in subsystems and transferred between them.

Consider a cylinder suspended in a reverberation room with loudspeakers placed inside the cylinder. The SEA model consists of three coupled systems as shown schematically in Fig. 2. The SEA model is that used by Crocker and Price [20]. The source or transmission room is the interior space of the cylinder and the receiving or reception room is the reverberant chamber in which the cylinder is located. The source and receiving rooms may be considered as systems 1 and 3, respectively and the cylinder as system 2. It is assumed that the flow of energy from one system to another is proportional to the modal energy difference [19]. Then the power balance equations of the three systems are [20]:

$$\Pi_1 = \omega(\eta_1 + \eta_{12} + \eta_{13})E_1 - \omega\eta_{21}E_2 - \omega\eta_{31}E_3, \tag{9a}$$

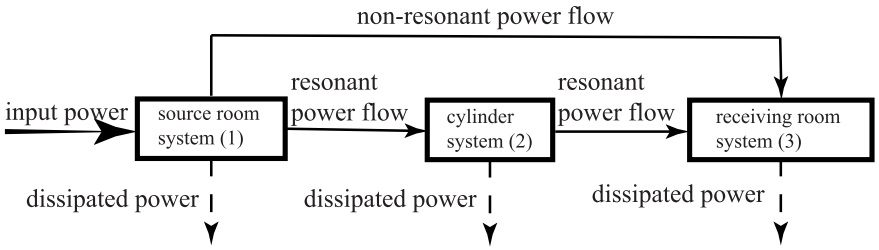

Fig. 2. Schematic of the SEA model.

$$\Pi_2 = -\omega\eta_{12}E_1 + \omega(\eta_2 + \eta_{21} + \eta_{23})E_2 - \omega\eta_{32}E_3, \tag{9b}$$

$$\Pi_3 = -\omega\eta_{13}E_1 - \omega\eta_{23}E_2 + \omega(\eta_3 + \eta_{31} + \eta_{32})E_3, \tag{9c}$$

where $\omega = 2\pi f$ is the circular frequency, η_i is the internal loss factor of system i, η_{ij} is the coupling loss factor between system i and system j, E_i is the total energy stored in system i and Π_i is the rate of energy flow into system i. It should be noted that the reciprocity relationship between coupling loss factor is used in obtaining power balance equations,

$$\eta_{ij}n_i = \eta_{ji}n_j, \tag{10}$$

where n_i and n_j are the modal densities of systems i and j, respectively. Therefore Eq. (9) can be written in matrix form as

$$\omega\begin{bmatrix} \eta_1 + \eta_{12} + \eta_{13} & -\eta_{21} & -\eta_{31} \\ -\eta_{12} & \eta_2 + \eta_{21} + \eta_{23} & -\eta_{32} \\ -\eta_{13} & -\eta_{23} & \eta_3 + \eta_{31} + \eta_{32} \end{bmatrix}\begin{Bmatrix} E_1 \\ E_2 \\ E_3 \end{Bmatrix} = \begin{Bmatrix} \Pi_1 \\ \Pi_2 \\ \Pi_3 \end{Bmatrix}. \tag{11}$$

The diagonal terms of the loss factor matrix are the total damping of each system. Since the cylinder is excited by driving a loudspeaker inside it, which is considered as system 1, the power flows Π_2 and Π_3 must equal zero; $\Pi_2 = 0$ and $\Pi_3 = 0$. Thus with this substitution and assuming that the loss factor of a system is larger than the coupling loss factors connecting it to other systems and ignoring the coupling loss factors in the total damping, Eq. (11) becomes

$$\omega\begin{bmatrix} \eta_1 & -\eta_{21} & -\eta_{31} \\ -\eta_{12} & \eta_2 & -\eta_{32} \\ -\eta_{13} & -\eta_{23} & \eta_3 \end{bmatrix}\begin{Bmatrix} E_1 \\ E_2 \\ E_3 \end{Bmatrix} = \begin{Bmatrix} \Pi_1 \\ 0 \\ 0 \end{Bmatrix}. \tag{12}$$

The SEA matrix is solved by inverting the coefficient matrix of Eq. (12) to give the energies in each systems. Hence, the ratio of energy in the source room (E_1) to the energy in the receiving room (E_3) can be obtained as

$$\frac{E_1}{E_3} = \frac{\eta_2\eta_3 - \eta_{23}\eta_{32}}{\eta_{12}\eta_{23} + \eta_2\eta_{13}}. \tag{13}$$

In order to obtain the noise reduction, following the procedure presented in Ref. [20], the unknown parameters of Eq. (13) must be calculated first. By using the reciprocity relationship, Eq. (10), Eq. (13) can be written as

$$\frac{E_1}{E_3} = \frac{\eta_2\eta_3 - (\frac{n_2}{n_3})\eta_{23}^2}{(\frac{n_2}{n_1})\eta_{21}\eta_{23} + \eta_2\eta_{13}}. \tag{14}$$

Here η_{21} and η_{23} are the coupling loss factors that account for sound radiation from the cylinder to the transmission and the reception spaces, respectively, which are given by Refs. [20,23]

$$\eta_{21} = \eta_{23} = \frac{\rho_a c_a \sigma_{\text{rad}}}{2\pi f \rho_c}, \tag{15}$$

where ρ_a is the density of air, ρ_c is the surface mass density of the cylinder and σ_{rad} is the radiation efficiency of the cylindrical shell.

2.3. Radiation efficiency

The radiation efficiency of a structure is a measure of how effectively its surface vibration leads to the radiation of sound to the acoustic field. It is defined as [1]

$$\sigma_{\text{rad}} = \frac{P}{\rho_a c_a S < v >^2}, \tag{16}$$

where P is the acoustic power radiated by the surface area S and $< v >^2$ is the spatially averaged mean square velocity on the radiating surface. The radiation efficiency for cylindrical shells can be estimated using the properties of acoustically fast (AF) and acoustically slow (AS) modes. Acoustically fast mode of a cylinder is defined as the mode for which the structural wavenumber is less than the acoustic wavenumber at the resonance frequency of the mode [32] which can be expressed as

$$k_l^2 + k_c^2 < k^2, \tag{17}$$

where k_l and k_c are the longitudinal wavenumber and circumferential wavenumber, respectively and k is the acoustic wavenumber. On the other hand, the converse is true for the acoustically slow mode which means that either the longitudinal wavenumber and/or the circumferential wavenumber are larger than the corresponding acoustic wavenumber. The cylinder's radiation efficiency can be calculated according to the frequency band of interest as follows.

The radiation efficiency in the case that only acoustically fast modes are present in the frequency band can be given as [44]

$$\sigma_{\text{rad}} = \frac{1}{[1 - \frac{(k_l^2 + k_c^2)}{k^2}]^{\frac{1}{2}}}. \tag{18}$$

Eq. (18) rapidly converges to unity, therefore it is approximated by $\sigma_{\text{rad}} \approx 1$.

Since the radiation efficiency is much higher for acoustically fast modes than for acoustically slow modes [20], in the case of existence of both acoustically fast and slow modes, all acoustically slow modes can be neglected. Thus, the radiation efficiency may be assumed to be given by the ratio of the number of acoustically fast modes (N_{AF}) in the frequency band to the total number of modes in the band (N).

$$\sigma_{\text{rad}} = \frac{N_{\text{AF}}}{N}. \tag{19}$$

The radiation efficiency for a frequency band that has solely acoustically slow modes which occurs for a cylinder with $f_r/f_c < 0.52$ in the frequency region $1 < f < f_c/f_r$ is given by Ref. [44]

$$\sigma_{\text{rad}} = \frac{(hR)^{\frac{1}{2}}[\ln(\frac{1+(\frac{f}{f_c})^{\frac{1}{2}}}{1-(\frac{f}{f_c})^{\frac{1}{2}}}) + \frac{2(\frac{f}{f_c})^{\frac{1}{2}}}{1-\frac{f}{f_c}}]}{\pi L[12(1-\nu^2)]^{\frac{1}{4}}(k_l^2 + k_c^2)^{\frac{1}{2}}(1-\frac{f}{f_c})^{\frac{1}{2}}}. \tag{20}$$

Oppenheimer and Dubowsky [45] introduced correction factors for sound radiation below the critical frequency of unbaffled plates with simply supported boundary conditions. These correction factors can be applied for cylindrical shells by knowing that there is no corner mode radiation for a cylindrically shaped structure. Therefore, the corrected radiation efficiency is given by

$$\sigma_{\text{rad}}^{\text{cor}} = F_{\text{cylinder}}\, F_{\text{edge}}\, \sigma_{\text{rad}}, \qquad f < f_c, \tag{21}$$

in which F_{cylinder} is the correction factor because of the effect of inertial flows that surround the cylinder at frequencies where the acoustic wavelength is more than the length of the cylinder, which is given by Ref. [45]

$$F_{\text{cylinder}} = \frac{53(\frac{f^4 S^2}{c_a^4})}{1 + 53(\frac{f^4 S^2}{c_a^4})}, \tag{22}$$

and F_{edge} is the local correction factor due to the effect on radiation from edge mode when the longitudinal wavenumber and/or the circumferential wavenumber is greater than the acoustic wavelength, which is given by Ref. [45]

$$F_{\text{edge}} = \frac{1}{2}\frac{49(\frac{f}{f_c})}{1 + 49(\frac{f}{f_c})}. \tag{23}$$

2.4. Loss factors

As mentioned in section 2.2, η_{21} and η_{23} are the coupling factors for the SEA model due to sound radiation from system 2 (cylinder structure) to system 1 (transmission space) and system 3 (reception room), respectively, which are calculated using Eq. (15). η_{13} is the coupling loss factor between two acoustical spaces (systems 1 and 3), which is obtained from Ref. [23]

$$\eta_{13} = \frac{c_a S}{8\pi f V_1}\tau_{13}, \tag{24}$$

in which V_1 is the volume that is occupied inside of the cylinder and τ_{13} is the mass law transmission coefficient, which is proportional to the mass of the cylinder and the frequency of incident acoustic wave. τ_{13} for random incident sound waves with different angles of incidence can be obtained by averaging the transmission coefficient for normal incidence over all possible incident angles [9]. The random incidence mass law transmission coefficient is then given by

$$\tau_{13} = \int_0^{\alpha} \frac{2\sin\alpha\cos\alpha}{(1+\frac{\pi f\rho_c}{2\rho_a c_a})^2}\,\mathrm{d}\alpha, \tag{25}$$

where α is the incidence angle. The integral interval for the diffuse sound field is chosen as $[0, 78°]$ [1,9,46].

η_3 is the dissipation loss factor of the reception chamber (system 3) that may be determined from the reverberation time method, which is given by Refs. [1,24]

$$\eta_3 = \frac{2.2}{fT_{60}}, \tag{26}$$

where T_{60} is the reverberation time of the chamber and can be calculated using following expression [1]

$$T_{60} = \frac{55.26V_3}{c_a S_3}, \tag{27}$$

in which V_3 and S_3 are the volume and the surface area of the reverberation chamber, respectively.

η_2 is the internal loss factor of the cylinder (system 2) due to radiation damping that can vary from 0.001 to 0.05 [43].

2.5. Sound transmission loss

The noise reduction (NR) of the sound pressure level from inside to outside of the cylindrical shell can be evaluated by taking the logarithm of Eq. (13), which yields

$$\mathrm{NR} = 10\log[\eta_2\eta_3 - (\frac{n_2}{n_3})\eta_{23}^2] - 10\log[(\frac{n_2}{n_1})\eta_{21}\eta_{23} + \eta_2\eta_{13}]. \tag{28}$$

where n_1 is the modal density of the acoustical space inside the cylinder which is introduced as the transmission room and is given by Ref. [20]

$$n_1 = \frac{2f^2V_1}{\pi c_a^3}, \tag{29}$$

n_3 is the modal density of the reverberation chamber (reception room), that for a room of volume V_3, surface area S_3 and total edge length P_3 is calculated by Ref. [19]

$$n_3 = \frac{4\pi f^2V_3}{c_a^3} + \frac{\pi f S_3}{2c_a^2} + \frac{P_3}{8c_a}, \tag{30}$$

and n_2 is the modal density of the cylinder structure that is obtained from: [47]

$$n_2 = \begin{cases} \dfrac{9\sqrt{3}L(\frac{f}{f_r})^{\frac{1}{2}}}{8\pi Rh} & f < f_r, \\ \dfrac{\sqrt{3}L}{2h} & f > f_r. \end{cases} \tag{31}$$

The transmission loss is then expressed by Ref. [25]

$$\mathrm{TL} = \mathrm{NR} + 10\log(\frac{1}{\mu} - \frac{3}{4}), \tag{32}$$

where μ is the absorption coefficient of the cylinder and enclosed air volume.

3. Experimental measurements

A thin-walled circular cylindrical shell was used for the experimental investigation and verification of the analytical results obtained. The following series of tests were carried out in a reverberant chamber:

- Measurement of the reverberation time, T_{60}, of the chamber.
- Measurement of the natural frequencies of the cylindrical shell.
- Measurement of the radiation efficiency of the cylinder structure.
- Measurement of the transmission loss of the cylindrical shell using two experimental methods: transmission suite method and sound intensity technique.
- Measurement of the noise reduction of the cylindrical shell with and without internal sound absorbing material.

The cylindrical shell used in the experiment was made of galvanized steel with material properties; Young's modulus $E = 200$ GPa, density $\rho = 7850\ \mathrm{kg/m^3}$ and Poisson's ratio $\nu = 0.28$. It had an outside diameter of 0.6 m with a wall thickness of 1.27 mm and overall length of 2.06 m. Two 19 mm wide plywood disks were inserted into both ends of the cylindrical shell and caused a 2.01 m length for the interior space of the cylinder. The disks were fastened tightly by several bolts throughout the cylinder. The disks were made of material sufficiently massive so sound transmission through them could be neglected. The cylinder was also completely sealed to prevent sound leakage. Therefore, the sound transmission was only considered through the cylindrical shell. It was suspended from the ceiling inside a cubic reverberation chamber, with sides of length 3.76 m, using nylon braided ropes and it contained two sets of loudspeakers and tweeters (Sony XS-R 1345) mounted at both ends inside the cylinder to the plywood disks. The loudspeakers covered low to high ranges of frequency (50 Hz–24000 Hz). In the experimental setup, a Brüel & Kjær microphone (type 4188 L1) was placed inside the cylinder in such a way that could be rotated by using a handle from outside. The outside and inside views of the test setup of the cylindrical shell as schematics are shown in Figs. 3 and 4, respectively.

3.1. Reverberation time of the reception room

The reverberation time of a room is defined as the time needed for the sound pressure level to drop by 60 dB from a steady level when a sound source is switched off [1,48]. It was of great importance to measure the reverberation time of the receiving room, since it was later used to calculate the sound transmission loss of the cylinder using the transmission suite method. The room was made of double walls of acoustically hard material with fiberglass filled in between them. The transmission suite room used in this study was mounted on air bags in order to prevent the transmission of vibration from the ground. Therefore, it was considered as a reverberation room with a sufficiently diffuse and reverberant sound field for doing the measurements. The reverberation time was measured using Brüel & Kjær Pulse system for one-twelveth octave frequency bands from 1 kHz to 12 kHz. Fig. 5 shows the reverberation time of the reception room.

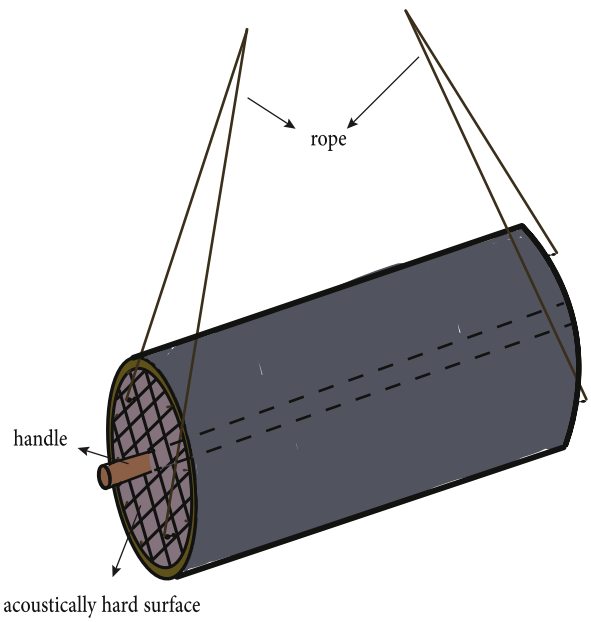

Fig. 3. Schematic of the setup, outside view.

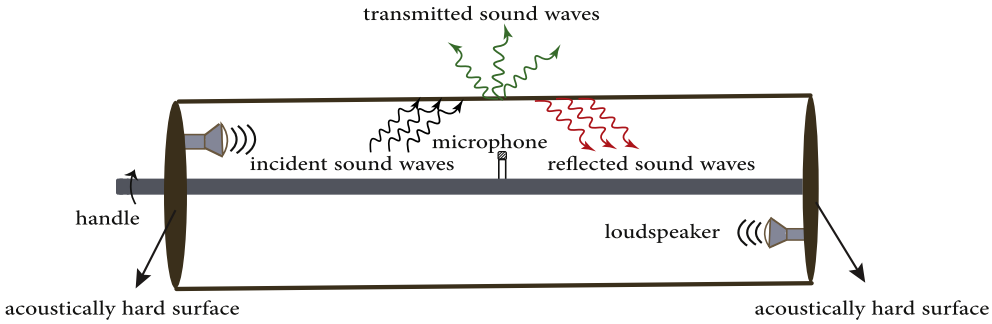

Fig. 4. Schematic of the setup, inside view.

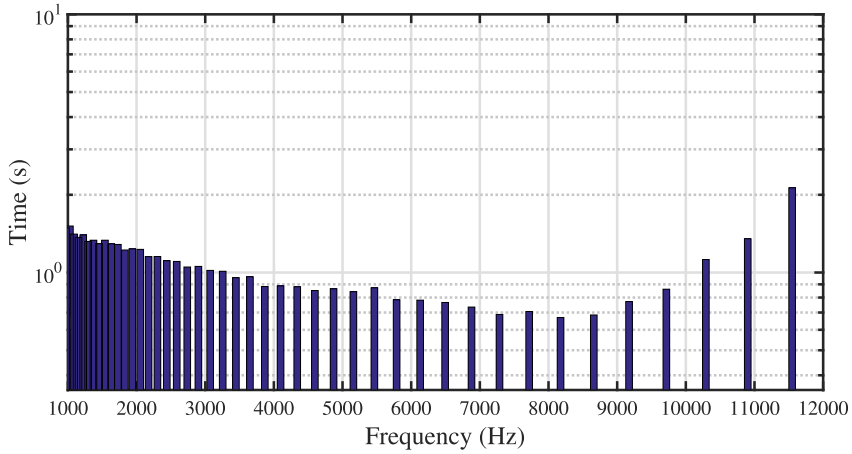

Fig. 5. Reverberation time of the reception room.

3.2. Validation of natural frequency calculations

In order to find natural frequencies of the cylinder, two methods of excitation were utilized; contact and non-contact excitation methods. For the contact approach, a modal hammer was used to excite natural frequencies of the cylinder and for the non-contact approach, loudspeakers inside the cylinder were used to excite resonance frequencies of the cylindrical shell. It should be considered that the mass and stiffness of the hammer tip are effective in improving the results obtained in the contact approach. The natural frequencies were measured by a Brüel & Kjær accelerometer (type 4375) in conjunction with a transducer. The measurements were analyzed using a Brüel & Kjær pulse multi-analyzer system (type 3560c). Fast Fourier Transforms (FFTs) obtained by each excitation methods are shown in Fig. 6. It is observed that the contact method could excite more natural frequencies in the frequency range 0–1000 Hz which can be considered as low frequency range and was not able to excite higher modes strongly enough and natural frequencies in medium and high ranges of frequency are barely noticeable in Fig. 6a. Unlike the hammer excitation technique which was only applicable for low frequency band, the non-contact method predicted natural frequencies in medium and high frequency bands as well as low frequency band. However, by comparing the peaks of FFT graphs in the frequency range 0–1000 Hz in Fig. 6a and b, it can be concluded that the hammer excitation technique is more effective in the low frequency range than the acoustical excitation technique because the peaks are more noticeable while for finding higher natural modes, the non-contact method is suggested.

In order to validate the expression presented for the natural frequency of a thin cylindrical shell based on the Soedel theory, the values of natural frequencies obtained theoretically compared with those obtained by two experimental techniques. The comparison is shown in Table 1. The mode number of each natural frequency were determined by analyzing the corresponding mode shape using MATLAB software. In order to obtain the mode shapes, several points were chosen over the perimeter of the cylinder along the longitudinal and circumferential directions. Results were extracted from Pulse software and were imported to the MATLAB software to analyze the mode shapes and determine the corresponding mode numbers. By knowing that the formula in Eq. (6) is an approximate closed form expression for the natural frequency of a thin cylindrical shell, the theory and measurements show good agreement. If more accurate values for the natural frequencies is needed, one can use the method presented by Oliazadeh et al. in Refs. [42,49]. However, a closed form solution cannot be acquired in the exact analysis.

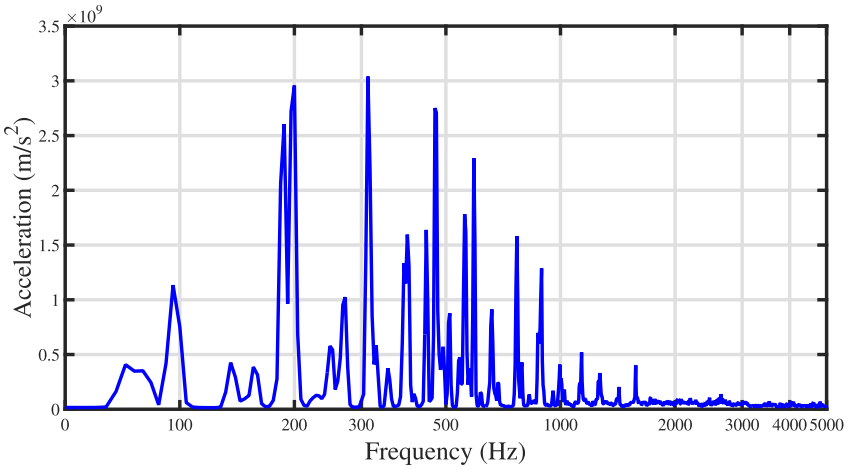

(a)

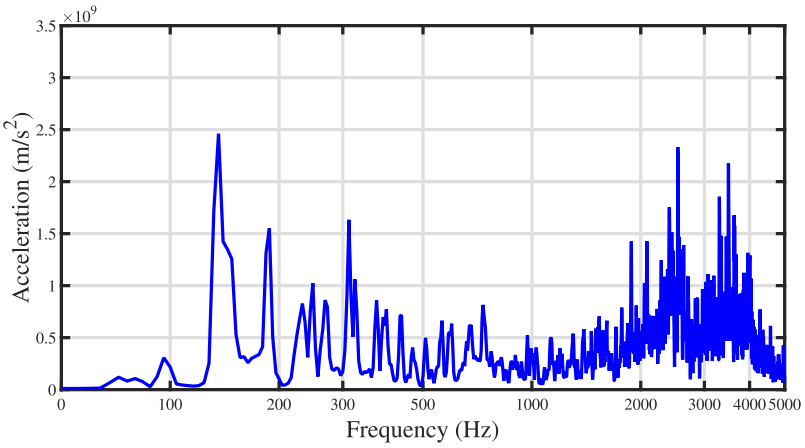

(b)

Fig. 6. FFT comparisons of two excitation methods: (a) Contact excitation; (b) Non-contact excitation.

Table 1
Comparison between experimental and theoretical results of natural modes in the frequency range 0–1000 Hz.

Mode Number		Natural Frequency (Hz)		
m	n	Contact method	Non-contact method	Theory
1	3	72	72	71
1	2	136	136	142
3	5	188	188	218
2	3	248	248	243
3	4	312	312	304
1	1	328	324	487
4	4	468	468	492
5	4	660	680	694
3	2	768	772	891
2	1	892	900	1256

3.3. *Radiation efficiency of the cylindrical shell*

As discussed in section 2.3, the radiation efficiency of the cylinder describes its acoustic radiation properties. In order to determine the radiation efficiency experimentally, it is necessary to measure the surface velocity of the vibrating structure and the acoustic power radiated by it. Therefore, another experiment on the cylindrical shell was conducted in the reverberation

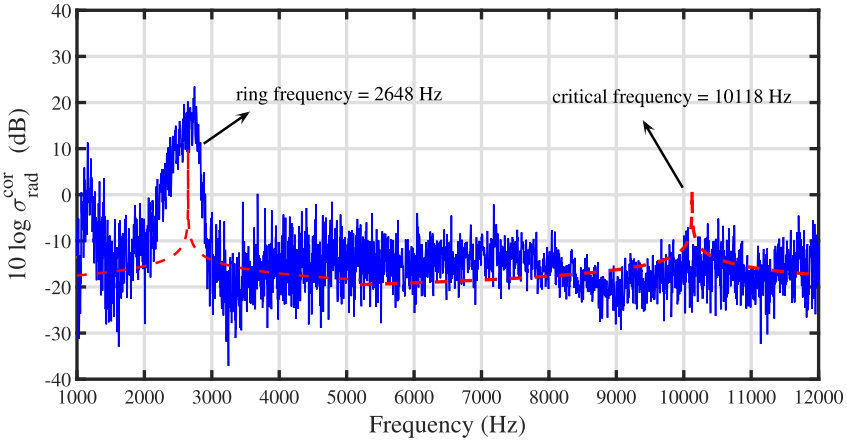

Fig. 7. Comparison of the experimental results of radiation efficiency (——) with analytical calculations (- - - - -).

chamber. The shell was excited by the loudspeakers inside the cylinder. The sound source propagated a random white noise signal which was generated by the Brüel & Kjær Pulse system. The acoustic power radiated was measured using a sound intensity probe scanned close over the surface of the cylinder. The probe (Brüel & Kjær, type 3599) comprised two 1/2 inch phase-matched microphones (type 4197) which were positioned face to face and separated by a 12 mm spacer (type UC-5269). The measurements and the scanning procedure were performed following the international standard ISO 15186-1. Simultaneously, the vibration data were taken at random locations over the cylindrical shell and then the mean square values at each frequency were averaged using the Brüel & Kjær accelerometer. The measured radiation efficiency is plotted in Fig. 7 and compared with the theoretical predictions.

It can be seen in Fig. 7 that the comparison of the experimental results with analytical calculations shows fairly good agreement. The corrected radiation efficiency is plotted in Fig. 7. For the cylinder under consideration, the analytical value of the ring and critical frequencies are 2648 Hz and 10118 Hz, respectively, therefore, the ratio f_r/f_c equals 0.26, which is less than one. Cylindrical shells with $f_r/f_c < 1$ are classified as acoustically thin shells [50]. For this kind of shell, the radiation efficiency has two peaks. First peak occurs at the ring frequency which is associated to the breathing mode resonance of the shell. Then the radiation efficiency decreases until it reaches the critical frequency at which the second peak appears and the structure radiates in a similar manner to a flat plate. Above the critical frequency, the radiation efficiency tends to unity by increasing the frequency and the logarithm value of that tends to zero. These features can be observed in the radiation efficiency measurements. The variation of the radiation efficiency values according to its definition (Eq. (16)) occurs between zero and one. Therefore, its logarithm varies between negative values and zero. The radiation efficiency of the cylindrical shell under consideration for frequencies below the ring frequency and between the ring and the critical frequency is between −10 dB and −20 dB and for frequencies above the critical frequency is −20 dB. This means that the cylindrical shell radiates poorly except at the ring frequency and the critical frequency which has a high radiation.

3.4. TL measurements of the cylindrical shell

The sound transmission loss of a structure may be evaluated by two experimental methods which are widely used by former researchers, namely transmission suite method and sound intensity method. In this paper, both methods are used to measure the transmission loss of the cylindrical shell and results are contrasted with analytical calculations.

3.4.1. Transmission suite method

The transmission suite method which is also referred as the two rooms method consists of two reverberant spaces called the transmission room and the reception room which are separated by the structure under investigation which is the thin cylindrical shell in the current paper. In this method, the TL is evaluated by measuring the sound pressure levels of the two spaces and the reverberation time of the reception room.

In order to measure the TL of the cylindrical shell by the transmission suite method a set of experiments was carried out in the reverberation chamber utilizing two Brüel & Kjær microphones (type 4188 L1) positioned inside and outside of the cylinder. The experimental setup is shown in Fig. 8. The sound field inside the cylinder was provided by the loudspeakers which is shown schematically in Fig. 4. The microphone placed inside the cylinder was rotated circumferentially during the measurements in order to achieve the spatially averaged sound pressure level in the circumferential direction. Fig. 9 shows the sound pressure levels inside the cylinder. It can be seen that the discrepancy between the measured sound pressure level at three different locations inside the cylinder with spatially averaged sound pressure level is less than 5 dB for the frequency range of interest. By knowing that the sound waves in a diffuse sound field are incident randomly from all directions and the magnitude of the

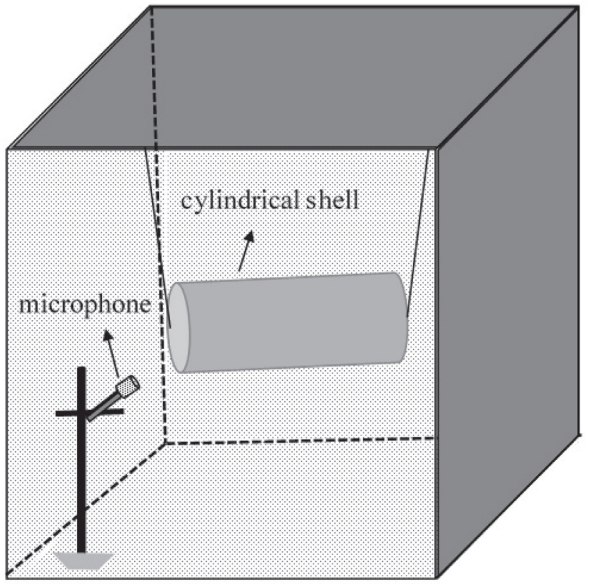

Fig. 8. Schematic display of the experimental setup for the TL measurement by transmission suite method.

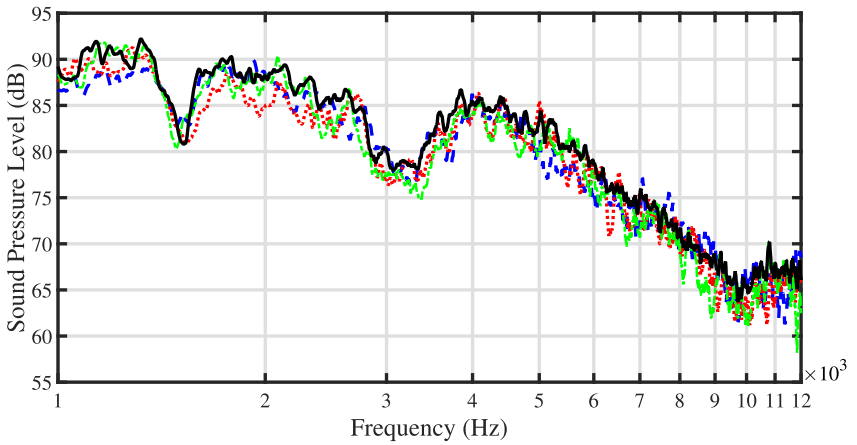

Fig. 9. Comparison of sound pressure levels between three points (- - - , ----- , -·-·-) with spatially averaged sound pressure level (——) inside the cylinder.

incident and reflected sound waves are the same provided the surface is rigid or heavy, the sound pressure level should be the same everywhere in a diffuse sound field. Therefore, by looking at the results shown in Fig. 9 which shows that the sound pressure level is approximately the same at any frequency regardless of orientation or location of the microphone, it can be concluded that the sound field inside the cylinder is sufficiently diffuse and the assumption of the reverberant room for the interior space of the cylindrical shell is acceptable. However, it is not always true the other way around. For example, a plane wave can also produce the same sound pressure level everywhere.

The noise reduction is obtained by subtracting the measured sound pressure level in the transmission room from the measured sound pressure level in the reception room. Then the transmission loss is acquired by taking into account the reverberation time which was measured previously, using the following expression [20]

$$\mathrm{TL} = \mathrm{NR} + 10\log[\frac{Sc_aT_{60}}{24V_3\ln(10)}]. \tag{33}$$

3.4.2. Sound intensity method

The second method used in order to evaluate the sound transmission loss of the cylindrical shell is the sound intensity technique. This method is based on determining the sound intensities inside and outside of the cylinder and calculating the

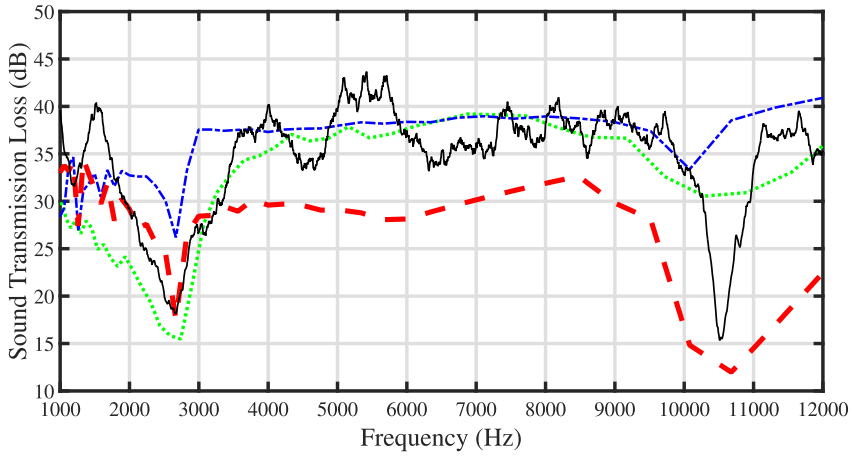

Fig. 10. Comparison between experimental and analytical results for sound transmission loss of the cylindrical shell; Current paper (- - -), Wang et al. [21] (-·-·-); Transmission suite method (.....) and Sound intensity method (——).

transmission loss using following expression [33]

$$\mathrm{TL} = 10\log(\frac{I_i}{I_t}), \tag{34}$$

where I_i and I_t are the incident and transmitted intensities, respectively.

Since the interior sound field is seen in Fig. 9 to be sufficiently diffuse, the incident intensity is calculated using the measured sound pressure results inside the cylinder which is given by Ref. [51]

$$I_i = \frac{p_{\mathrm{rms}}^2}{4\rho_a c_a}. \tag{35}$$

where p_{rms} is the measured average sound pressure inside the cylinder. By knowing that the sound field in the receiving room was sufficiently diffuse, the transmitted intensity was measured by moving the sound intensity probe over the surface of the cylinder.

3.4.3. Comparison of two methods of measuring sound transmission loss

Fig. 10 shows the sound transmission loss of the cylindrical shell obtained by the two experimental methods. The internal sound pressure levels provided by the loudspeakers were held constant for both experimental methods and also during the measurements. The transmission loss measured by the transmission suite method is plotted in one-twelveth octave frequency bands. Since the reverberation time was measured in one-twelveth octave bands, the transmission loss must be plotted in the same frequency band. As expected, it shows two recognizable dips in the transmission loss curve. The first dip occurs at the ring frequency which is predicted at 2738 Hz. Above the ring frequency, the transmission loss increases up to the critical frequency where the second dip is observed at 10290 Hz. The percentage of error between predicted and calculated ring frequencies is 3.0% and that for the critical frequency is 1.7% which is indicative of a good agreement between the experimental and theoretical evaluations.

In the second method the transmitted intensity through the cylinder was measured by moving the intensity probe over the entire cylindrical shell surface. It can be seen from Fig. 10 that the transmission loss obtained by the sound intensity method shows a similar trend to the results obtained by the transmission suite technique. The ring and critical frequencies are predicted at 2600 Hz (1.8% error) and 10530 Hz (4.1% error), respectively which represents a good agreement between the experimental and analytical predictions.

A comparison is also made between the experimental measurements of the transmission loss of the cylindrical shell and theoretical SEA calculations of the present study and the work done by Wang et al. [21] which is plotted in Fig. 10. It shows that the agreement between the analytical result of the current paper and experimental measurements is better than the Wang's result in the low frequency region and specifically at the ring frequency. The reason is that two correction factors have been used for the radiation efficiency which are effective in low frequencies. The agreement between two experimental methods is poor for the low frequency region below the ring frequency. It can be due to the fact that in the sound intensity method, the incident intensity was obtained using the measured sound pressure results (Eq. (35)) based on the assumption of a diffuse sound field inside the cylinder. Although it is assumed that the sound field of the interior space of the cylinder is diffuse, this assumption in the low frequency region is not as reliable as the assumption for the medium and high frequency regions. Because the sound pressure levels for three random locations displayed in Fig. 9 showed dissimilarity in the low frequencies which may be the cause for the inconsistency between two experimental methods at low frequency region.

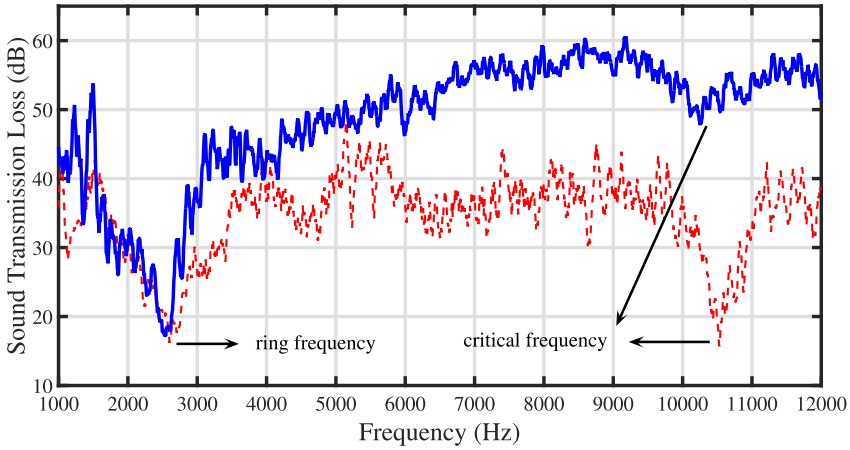

Fig. 11. Comparison of measured transmission loss with (——) and without (- - - -) absorbing material using sound intensity method.

As it was observed in Fig. 10, both experimental techniques, the transmission suite method and the sound intensity method, agree very well in the medium and high frequency regions, between the ring and critical frequencies. At frequencies higher than the critical frequency, the sound intensity measurement was not reliable since the sound intensity probe failed at frequencies above 12 kHz. For frequencies between the ring and critical frequencies, Wang's theoretical results yields better agreement and about 5 dB to 10 dB discrepancy is observed between the results of the present study and Wang's paper. This can be due to ignoring coupling loss factors in comparison with total damping in the derivation of the noise reduction expression which causes a decrement in the transmission loss trend in medium and high frequency regions. However, the analytical result of the current paper predicts the sound transmission loss better than the Wang's result at the critical frequency.

4. Effects of using sound absorbing material

In the previous section, the experimental measurements of sound transmission loss are compared with the theoretical results. The value of the internal loss factor of the cylinder, η_2, and its absorption coefficient, μ, used in the analytical calculations according to the setup conditions when the cylinder was not lined with any absorbing materials was 0.05 and 0.001, respectively.

It is of interest to study the effect of absorbing material such as fiberglass. As mentioned in the literature review, different approaches have been applied in order to achieve better noise transmission characteristics with cylindrical shells. Adding absorbing material such as fiberglass inside the cylinder is a suitable way to improve the noise reduction without a significant change in the weight of the structure and its vibrational response. Therefore, another experiment was carried out with fiberglass inside the cylinder. In the experiment, fiberglass was placed around the longitudinal axis of the cylinder.

It is helpful to compare the sound transmission loss measured with the absorbing material inserted into the cylinder and without it. The comparison is shown in Fig. 11. It is observed that utilizing absorbing material has positive effects on the noise

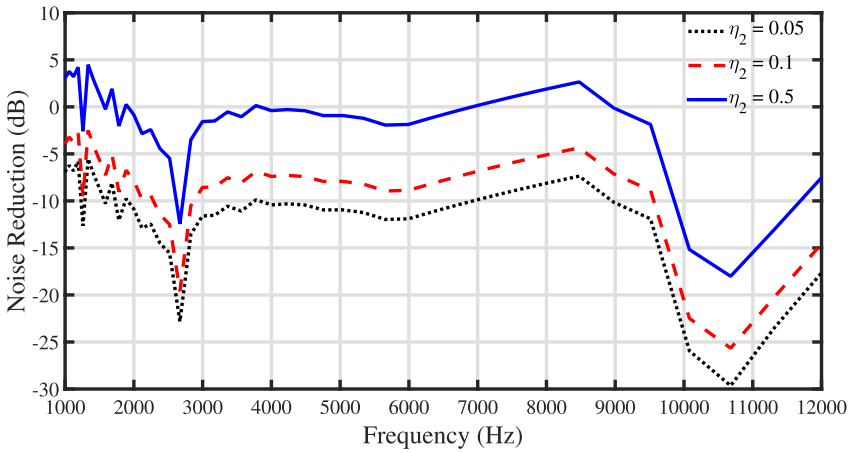

Fig. 12. Theoretical effect of absorption coefficient on noise reduction of a cylindrical shell.

reduction of the cylindrical shell specially at high frequencies. The noise reduction is increased about 15 dB in high frequency bands and 35 dB at critical frequency which is a great achievement because sound transmits easily through a structure at its critical frequency, therefore obtaining high transmission loss at this specific frequency is vital from the acoustical point of view. The effect of absorption coefficient on the noise reduction is shown in Fig. 12. It can be concluded that use of absorbing material with a higher absorption coefficient gives a better noise reduction performance.

5. Conclusions

In this paper an analytical model was developed based on statistical energy analysis (SEA) theory to investigate the acoustic behavior of a thin-walled circular cylindrical shell. The noise reduction and sound transmission loss were obtained theoretically for a finite shell model. The effects of internal loss factors were considered in the derivation. An experiment was also carried out in a reverberation chamber in order to measure the transmission loss and compare it with the analytical results. First, natural frequencies of the shell were measured using two excitation methods, contact method in which a modal hammer was used and non-contact method which included an acoustical excitation using loudspeakers. It was found out that the contact method was more efficacious in low frequency region and the non-contact method was able to excite higher natural modes much better than the other method. A simplified expression for natural frequency based on Soedel theory was presented in the theoretical part. The calculated natural frequencies were also compared with the experimental results and showed fairly good agreement. One of the important SEA parameters is the radiation efficiency which was measured separately. Good agreement was obtained by comparing the experimental results with those calculated using the expression presented for the corrected radiation efficiency.

The sound transmission loss of the cylindrical shell were measured using two experimental techniques, the transmission suite method and the sound intensity method. The experimental results were contrasted with transmission loss values calculated using the SEA theory. It was observed that the analytical approach of obtaining sound transmission loss produced better results in the low frequency region than the medium and high frequency regions, which is because of applying correction factors at low frequencies. The analytical result showed good agreement with the experimental methods at the ring and critical frequencies. The errors between calculated values for the ring and critical frequencies and predicted ones were less than 4.1% which is a satisfactory outcome. The experimental methods were also compared together which indicated some discrepancies in low frequency region but they agreed very well in the medium and high frequency regions, between the ring and critical frequencies. It is mainly because of the assumption of diffuse sound field for the interior space of the cylinder. The interior noise level was almost reverberant at medium and high frequencies but it was not completely diffuse at low frequencies. Therefore, the sound intensity method which obtained the incident intensity using the measured sound pressure levels based on the assumption of a diffuse sound field, had some discrepancies in transmission loss results with those from the transmission suite method at low frequencies.

The effects of absorbing material on the acoustic behavior of the cylindrical shell were also investigated using the analytical solutions and experimentally. It was found out that using sound absorbing material such as fiberglass inside the cylinder improved its acoustical behavior at the critical frequency. Therefore, considering the light weight of fiber glass and its performance, it is seen to be a good way to improve noise reduction in thin-walled cylindrical shells.

Appendix

The coefficients in Eq. (3) are expressed as follows:

$$C_{11} = -\lambda^2 R^2 - \frac{1-\nu}{2} n^2 - \frac{\rho(1-\nu^2)}{E} R^2 \omega_{mn}^2$$

$$C_{12} = \frac{1+\nu}{2} n\lambda R$$

$$C_{13} = \nu \lambda R$$

$$C_{22} = -(1+\beta)\left(\frac{1-\nu}{2}\lambda^2 R^2 + n^2\right) - \frac{\rho(1-\nu^2)}{E} R^2 \omega_{mn}^2$$

$$C_{23} = -n[1 + \beta(\lambda^2 R^2 + n)]$$

$$C_{33} = 1 + \beta(\lambda^2 R^2 + n^2)^2 - \frac{\rho(1-\nu^2)}{E} R^2 \omega_{mn}^2$$

References

[1] M.J. Crocker, Handbook of Noise and Vibration Control, John Wiley & Sons, New Jersey, 2007.
[2] L.R. Koval, On sound transmission into a thin cylindrical shell under "flight conditions", J. Sound Vib. 48 (1976) 265–275.
[3] L.R. Koval, Effects of cavity resonances on sound transmission into a thin cylindrical shell, J. Sound Vib. 59 (1978) 23–33.
[4] L.R. Koval, Sound transmission into a laminated composite cylindrical shell, J. Sound Vib. 71 (1980) 523–530.
[5] A. Blaise, C. Lesueur, M. Gotteland, M. Barbe, On sound transmission into an orthotropic infinite shell: comparison with koval's results and understanding of phenomena, J. Sound Vib. 150 (1991) 233–243.
[6] A. Blaise, C. Lesueur, Acoustic transmission through a 2-d orthotropic multi-layered infinite cylindrical shell, J. Sound Vib. 155 (1992) 95–109.
[7] J.H. Lee, J. Kim, Analysis and measurement of sound transmission through a double-walled cylindrical shell, J. Sound Vib. 251 (2002) 631–649.

[8] J.H. Lee, J. Kim, Sound transmission through periodically stiffened cylindrical shells, J. Sound Vib. 251 (2002) 431–456.
[9] J.H. Lee, J. Kim, Study on sound transmission characteristics of a cylindrical shell using analytical and experimental models, Appl. Acoust. 64 (2003) 611–632.
[10] J. Zhou, A. Bhaskar, X. Zhang, Optimization for sound transmission through a double-wall panel, Appl. Acoust. 74 (2013) 1422–1428.
[11] J. Zhou, A. Bhaskar, X. Zhang, The effect of external mean flow on sound transmission through double-walled cylindrical shells lined with poroelastic material, J. Sound Vib. 333 (2014) 1972–1990.
[12] Y. Liu, C. He, On sound transmission through double-walled cylindrical shells lined with poroelastic material: comparison with zhou s results and further effect of external mean flow, J. Sound Vib. 358 (2015) 192–198.
[13] Y. Liu, C. He, Diffuse field sound transmission through sandwich composite cylindrical shells with poroelastic core and external mean flow, Compos. Struct. 135 (2016) 383–396.
[14] Y. Liu, C. He, Analytical modelling of acoustic transmission across double-wall sandwich shells: effect of an air gap flow, Compos. Struct. 136 (2016) 149–161.
[15] Y. Liu, A. Sebastian, Effects of external and gap mean flows on sound transmission through a double-wall sandwich panel, J. Sound Vib. 344 (2015) 399–415.
[16] Y. Liu, Sound transmission through triple-panel structures lined with poroelastic materials, J. Sound Vib. 339 (2015) 376–395.
[17] P. Oliazadeh, A. Farshidianfar, Analysis of different techniques to improve sound transmission loss in cylindrical shells, J. Sound Vib. 389 (2017) 276–291.
[18] G. Maidanik, Response of ribbed panels to reverberant acoustic fields, J. Acoust. Soc. Am. 34 (1962) 809–826.
[19] R.H. Lyon, Statistical Energy Analysis of Dynamical Systems: Theory and Applications, MIT Press, Cambridge, 1975.
[20] M.J. Crocker, A.J. Price, Sound transmission using statistical energy analysis, J. Sound Vib. 9 (1969) 469–486.
[21] Y.S. Wang, M.J. Crocker, P.K. Raju, Theoretical and experimental evaluation of transmission loss of cylinders, AIAA J. 21 (1983) 186–192.
[22] E. Reynders, R.S. Langley, A. Dijckmans, G. Vermeir, A hybrid finite element–statistical energy analysis approach to robust sound transmission modeling, J. Sound Vib. 333 (2014) 4621–4636.
[23] C. Churchill, C. Hopkins, Prediction of airborne sound transmission across a timber–concrete composite floor using statistical energy analysis, Appl. Acoust. 110 (2016) 145–159.
[24] Y.K. Tso, C.H. Hansen, An investigation of the coupling loss factor for a cylinder/plate structure, J. Sound Vib. 199 (1997) 629–643.
[25] E. Szechenyi, Sound transmission through cylinder walls using statistical considerations, J. Sound Vib. 19 (1971) 83–94.
[26] R.S. Langley, The modal density and mode count of thin cylinders and curved panels, J. Sound Vib. 169 (1994) 43–53.
[27] F.W. Williams, J.R. Banerjee, Accurately computed modal densities for panels and cylinders, including corrugations and stiffeners, J. Sound Vib. 93 (1984) 481–488.
[28] P. Ramachandran, S. Narayanan, Evaluation of modal density, radiation efficiency and acoustic response of longitudinally stiffened cylindrical shell, J. Sound Vib. 304 (2007) 154–174.
[29] S.J.K. Florence, K. Renji, Modal density of thin composite cylindrical shells, J. Sound Vib. 365 (2016) 157–171.
[30] P. Hynna, P. Klinge, J. Vuoksinen, Prediction of structure-borne sound transmission in large welded ship structures using statistical energy analysis, J. Sound Vib. 180 (1995) 583–607.
[31] R.J.M. Craik, R. Wilson, Sound transmission through parallel plates coupled along a line, Appl. Acoust. 49 (1996) 353–372.
[32] D. Chronopoulos, B. Troclet, M. Ichchou, J.P. Lainé, A unified approach for the broadband vibroacoustic response of composite shells, Compos. B Eng. 43 (2012) 1837–1846.
[33] R.E. Halliwell, A.C.C. Warnock, Sound transmission loss: comparison of conventional techniques with sound intensity techniques, J. Acoust. Soc. Am. 77 (1985) 2094–2103.
[34] A. De Mey, R.W. Guy, Exploiting the laboratory measurement of sound transmission loss by the sound intensity technique, Appl. Acoust. 20 (1987) 219–236.
[35] H. Fukuhara, Evaluation of sound insulation materials in a reverberant field by the sound intensity method, Appl. Acoust. 24 (1988) 169–191.
[36] J.C.S. Lai, D. Qi, Sound transmission loss measurements using the sound intensity technique part 1: the effects of reverberation time, Appl. Acoust. 40 (1993) 311–324.
[37] Y.H. Chen, K.T. Chen, Y.H. Chaing, Plate-damping measurements in a single reverberation room, Appl. Acoust. 47 (1996) 251–261.
[38] G.R. Watts, In situ method for determining the transmission loss of noise barriers, Appl. Acoust. 51 (1997) 421–438.
[39] M. Praščević, D. Cvetković, D. Mihajlov, Comparasion of prediction and measurement methods for sound insulation of lightweight partitions, FU Arch. Civ. Eng. 10 (2012) 155–167.
[40] M. Connelly, M. Hodgson, Experimental investigation of the sound transmission of vegetated roofs, Appl. Acoust. 74 (2013) 1136–1143.
[41] V.N. Koukounian, C.K. Mechefske, Computational modelling and experimental verification of the vibro-acoustic behavior of aircraft fuselage sections, Appl. Acoust. 132 (2018) 8–18.
[42] P. Oliazadeh, M.H. Farshidianfar, A. Farshidianfar, Exact analysis of resonance frequency and mode shapes of isotropic and laminated composite cylindrical shells; part i: analytical studies, J. Mech. Sci. Technol. 27 (2013).
[43] F.J. Fahy, P. Gardonio, Sound and Structural Vibration: Radiation, Transmission and Response, Academic Press, London, 2007.
[44] E. Szechenyi, Modal densities and radiation efficiencies of unstiffened cylinders using statistical methods, J. Sound Vib. 19 (1971) 65–81.
[45] C.H. Oppenheimer, S. Dubowsky, A radiation efficiency for unbaffled plates with experimental validation, J. Sound Vib. 199 (1997) 473–489.
[46] J. Jung, J. Kook, S. Goo, S. Wang, Sound transmission analysis of plate structures using the finite element method and elementary radiator approach with radiator error index, Adv. Eng. Software 112 (2017) 1–15.
[47] F.D. Hart, K.C. Shah, Compendium of Modal Densities for Structures, NASA, 1971.
[48] M. Möser, Engineering Acoustics: an Introduction to Noise Control, Springer Science & Business Media, Berlin Heidelberg, 2009.
[49] P. Oliazadeh, M.H. Farshidianfar, A. Farshidianfar, Exact analysis of resonance frequency and mode shapes of isotropic and laminated composite cylindrical shells; part ii: parametric studies, J. Mech. Sci. Technol. 27 (2013) 3645–3649.
[50] C. Wang, J.C.S. Lai, The sound radiation efficiency of finite length acoustically thick circular cylindrical shells under mechanical excitation i: theoretical analysis, J. Sound Vib. 232 (2000) 431–447.
[51] M.J. Crocker, P.K. Raju, B. Forssen, Measurement of transmission loss of panels by the direct determination of transmitted acoustic intensity, Noise Contr. Eng. 17 (1981) 6–11.